Three Classes of Morphology Transitions in the Solidification of a Liquid Crystal

Jeffrey L. Hutter* and John Bechhoefer

Department of Physics, Simon Fraser University, Burnaby, British Columbia, V5A 1S6, Canada

(Received 5 May 1997)

We have studied growth morphologies during solidification of a liquid crystal (10 OCB). As the undercooling is varied, sharp transitions analogous to equilibrium phase transitions are seen between the growth modes. We identify three types of morphology transitions: strongly first order, where the growth velocity is discontinuous at the transition; weakly first order, where the velocity curve, but not its derivative, is continuous and the morphology changes discontinuously; and second order, with continuous changes in the growth properties and pretransitional effects. [S0031-9007(97)04519-5]

PACS numbers: 81.10.Aj, 64.70.Md, 81.30.Fb

Solidification morphologies depend greatly on the initial fluid undercooling and on the crystalline anisotropy [1]. In different regimes, there are dendrites, compact and fractal "seaweed" [1], and spherulites [2,3]. How does one morphology transform into another as the undercooling ΔT is varied? One possibility is that there is a smooth crossover, where all quantities vary analytically with ΔT. In metals [4] and polymers [5], theories of kinetics-limited growth, where the rate of freezing is limited by local attachment kinetics, typically predict such crossovers. Another possibility is that morphologies may vary nonanalytically with ΔT, in analogy with equilibrium phase transitions [1,6–8]. Different morphologies are then the result of distinct growth mechanisms which may coexist at a given undercooling ΔT. Ben-Jacob *et al.* have classified such morphology transitions according to the behavior of the average front velocity v at the transition [6]. They identified transitions accompanied by a jump in growth velocity as first order, while those with a continuous velocity curve $v(\Delta T)$ and a discontinuity in slope were termed second-order morphology transitions.

Although multiple growth morphologies have been seen in many systems, there are fewer experimental studies of the transitions. Sharp transitions have been seen experimentally in metals [9], electrochemical deposition [10], and Hele-Shaw cells [6,11]. However, most of these studies, as well as theoretical discussions [1,7,8], have dealt with solidification in the diffusive regime, where growth is limited by diffusion of latent heat or impurities away from the front of the advancing solid phase. Here, we observe solidification morphology transitions in both the diffusive and kinetic limits. We then show that a slope discontinuity in the $v(\Delta T)$ curve need not imply a second-order transition. Finally, we present evidence for the first observation of a true second-order morphology transition.

We have recently begun to study the (nearly) isothermal solidification of the liquid crystal 4-cyano-4′-decyloxybiphenyl (10 OCB) into a true crystalline solid [12,13]. We observe at least six distinct morphologies, illustrated in Fig. 1, as a function of the undercooling (the difference between the equilibrium melting point, 59.5 °C, and the growth temperature). Although the solidification is from the smectic-*A* phase, the liquid crystalline properties appear to be unimportant [12], and similar morphologies are seen in a variety of materials. The main reason for our choice of solidification system is one of convenience: morphology transitions occur with front velocities of 10–100 μm/s, which is slow enough to observe growth dynamics (in contrast to metals, where transitions occur typically at meters per second), but fast enough that a large number of experiments can be performed (in contrast with polymers where transitions occur typically at less than 1 μm/s). Moreover, 10 OCB can be easily undercooled, allowing ready access to the kinetic regime.

In Fig. 2, measurements of the front velocity for 10 OCB show that most of the morphologies in Fig. 1 are separated by singular points in the $v(\Delta T)$ curve. One exception is the crossover between modes *B* and *C*. Experimentally, the velocity curve is smooth to our resolution—there is a continuous evolution between the faceted needle crystals of mode *B* and the sidebranched dendrites of mode *C*. Physically, the transition is caused by kinetic roughening of faceted surfaces [14].

Sharp transitions are also seen. For instance, the large jump in velocity clearly identifies the transitions involving mode B' as first-order morphology transitions. As can be seen from Fig. 2, other growth modes are occasionally observed at undercoolings where mode B' can exist. This is evidence of hysteresis in the transitions: the metastable solutions are separated from the mode B' solution by "barriers" large enough to make nucleation of mode B' infrequent.

The velocity curve, but not its derivative, is continuous at the transition between modes *C* and *D*, which occurs near $\Delta T = 15$ °C. According to the nomenclature of Ben-Jacob *et al.*, this would be termed a second-order transition. However, the transition is accompanied by a sudden change in structure and interface roughness [12]. This jump in growth form suggests that the *CD* transition is first order, despite the continuous velocity curve.

Clearer indications that the *CD* transition is first order are provided by its dynamics: if the undercooling during mode-*D* growth is decreased to a value that favors

 0031-9007/97/79(20)/4022(4)$10.00

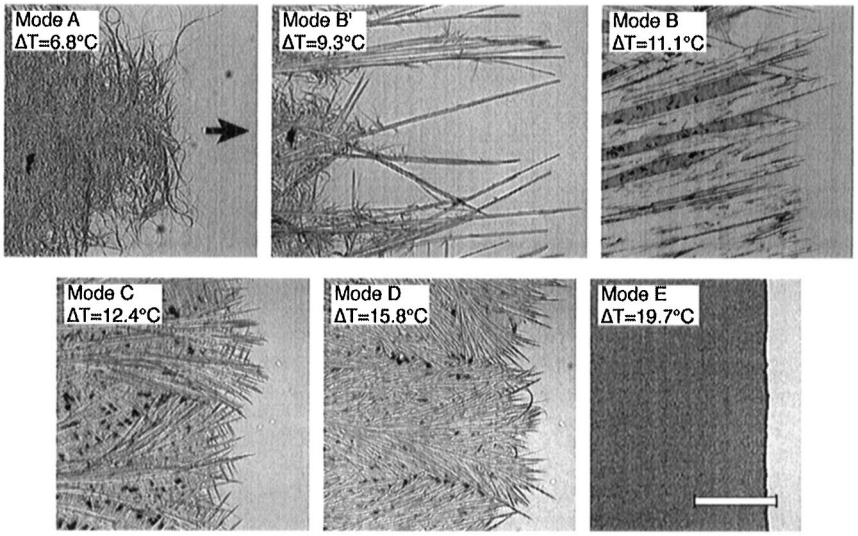

FIG. 1. Growth morphologies of modes $A-E$. The scale bar represents 200 μm. The front is advancing to the right in all cases, as indicated by the arrow. (See Fig. 4 for images of mode F.)

mode C, the transition occurs by the nucleation and subsequent lateral expansion of mode C (and vice versa). In Fig. 3(a), a region of mode C has nucleated after a sudden decrease in undercooling (from $\sim$16 to $\sim$14 °C) during growth of a mode-D front. The mode-C front will eventually spread laterally to cover the original mode D. The lack of hysteresis in the phase diagram—and the lack of any evidence that the two morphologies are becoming more similar—prompts us to term this transition weakly first order, in contrast to the strongly first-order AB' and $B'B$ transitions. Here, the noise is large enough relative to any barriers that the new mode nucleates once the stability threshold is crossed.

Further evidence that C and D represent distinct growth modes, with separate velocity curves, rather than a single growth mechanism with a strong dependence on undercooling, is provided by the reentrance of mode D at small undercoolings (see the filled-in symbols near $\Delta T = 10$ °C in Fig. 2). This observation is consistent with a mechanism for mode D that can exist over a large range of undercoolings but is only selected in parts of the range (the B/C mechanism is selected at intermediate undercoolings). Ben-Jacob *et al.* have hypothesized that the fastest-growing mode will be selected in such cases [6]. Both of the transitions between modes D and B/C, as well as the DE transition (which will not be discussed here), favor the

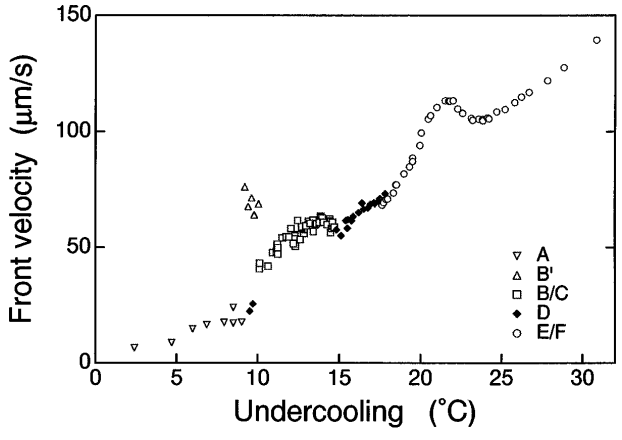

FIG. 2. Growth velocity as a function of undercooling for 10 OCB. We label the different branches of the curve $A-F$ and identify them with the distinct growth modes illustrated in Fig. 1. The uncertainties are typically less than 1 μm/s in velocity and 0.5 °C in undercooling (after correction for the finite conductivities of the sample and glass plates). Note that the transition between modes B and C is not sharp. The EF transition is discussed in greater detail in Fig. 5.

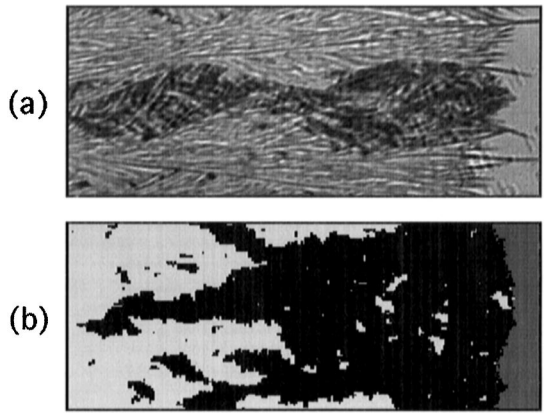

FIG. 3. Mode nucleation. Growth is to the right in both cases. (a) The D-C transition. The darker region is a portion of mode C that has nucleated and is spreading outward at the expense of mode D. The image measures 300 $\times$ 750 μm. (b) Simulation of mode nucleation (100 $\times$ 250 lattice spacings). The mode with the larger growth velocity (darker regions) is able to take over the growth front, once it has nucleated. Growth probabilities are $P_S = 10^{-3}$, $P_C = 0.207$, and $P_D = 0.2$ (see text).

faster mode. Indeed, the observation of a mode transition at precisely the undercooling where two unrelated velocity curves cross is strong evidence that the selection principle in this case is a function of velocity alone.

To show how a continuous velocity curve can be compatible with a first-order morphology transition, we introduce a variant of a simple lattice model discussed by Saito *et al.* [8] Consider a square lattice where each point can be in one of three states, corresponding to modes C, D, and the smectic (represented by -1, $+1$, and 0 in the computer). The initial conditions are a column of $+1$'s (all mode D) with everywhere else smectic. During each time step, every solid site that has a smectic nearest neighbor—an "interface" site, for short—can grow. We pick each interface site. If the solid is mode D, look at each nearest neighbor, and convert the smectic to mode D with probability P_D and to mode C with probability P_S ("S" for "switch"). Let it remain smectic with probability $(1 - P_D - P_S)$. Typically, $P_D \approx 20\%$ and $P_S = 0.1\%$. If the site is mode C, the open nearest neighbors are converted to C with probability P_C, to D with probability P_S, and left unchanged with probability $1 - P_C - P_S$. Again, $P_C \approx 20\%$. Although extremely simple, this model captures a number of features of kinetics-limited growth: It is purely *local.* It allows and generates overhangs, as seen in experiments. The overall front is rough on smaller scales but does not show the shape instabilities of the diffusive regime. The key feature of the model, though, is the small probability to hop back and forth from modes D to C and vice versa. When the growth probability (which is proportional to the front velocity) of mode C is less than that of mode D (i.e., $P_C < P_D$), domains of C nucleate but then die away. When $P_C = P_D$, large domains of D and C alternate. When $P_C > P_D$, an initially uniform domain of D quickly converts to C. [See Fig. 3(b).] With enough patience, an arbitrarily small velocity difference will let the faster mode take over. Thus, the velocity curve can remain continuous experimentally, even though modes C and D are not particularly "close" to each other.

So far, we have discussed modes with fairly open front shapes, identifying them (with the possible exception of mode D) as diffusion-limited modes. We now consider the transition between mode E and mode F. These are normal and banded spherulites and are typical of growth in the kinetic regime [2,3]. Figure 4 shows the evolution in growth morphology, which occurs near the local growth velocity maximum shown in Figs. 2 and 5(a). Approaching the transition from the banded side, the wavelength of the bands diverges while their order sharply decreases. [See Figs. 5(b) and 5(c).] The disorder in the bands reflects the increasing importance of fluctuations near the transition. The band amplitude, as measured by intensity profiles [right-hand side and insets of Fig. 5(d)], also diverges at an undercooling near 22 °C. Similarly, measurements of the image contrast in the nonbanded (mode E) regime also show a rapid increase near this undercooling [left-hand side of Fig. 5(d)].

The nature of the EF transition remains elusive. The sudden change in correlation length suggests an order-disorder transition [15], but the amplitude of the bands clearly does not vanish at this point, contrary to expectation. On the other hand, the diverging wavelength and "solitonlike" intensity traces suggest a continuous nucleation transition [16], the archetype of which is the unwinding transition of a cholesteric liquid crystal in an external field. (Near such transitions, domain sizes diverge logarithmically and domains are separated by narrow twist walls. The latter is consistent with our observation

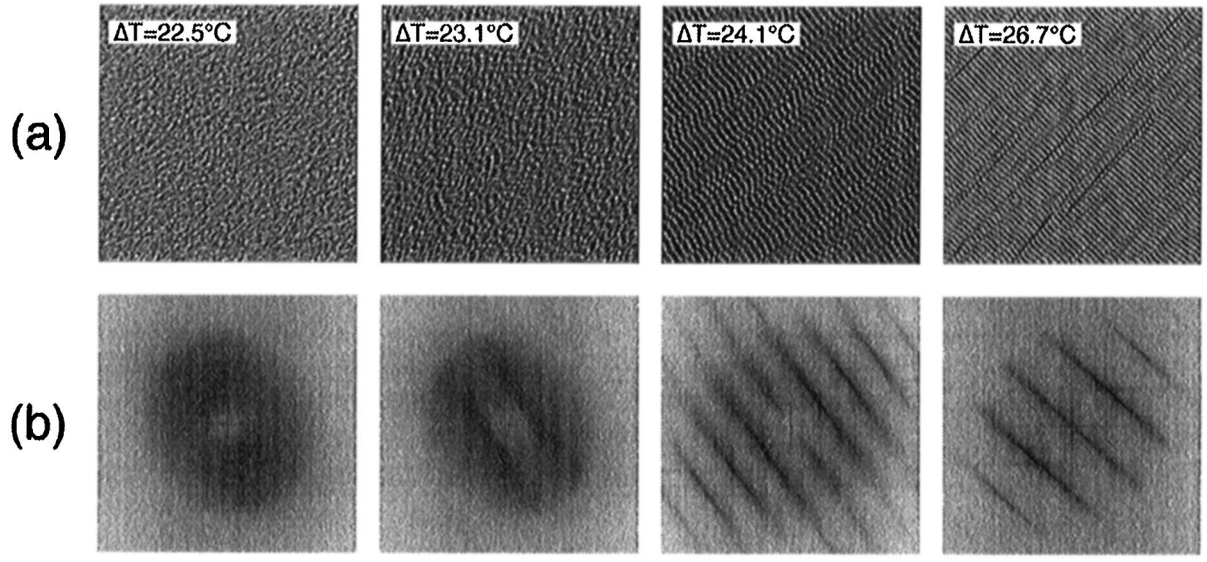

FIG. 4. Growth morphologies at the EF transition. (a) Structure of the solid at undercoolings spanning the transition. Growth was to the upper right in all cases. Each image measures 120 μm square. (b) Power spectral density of images in (a).

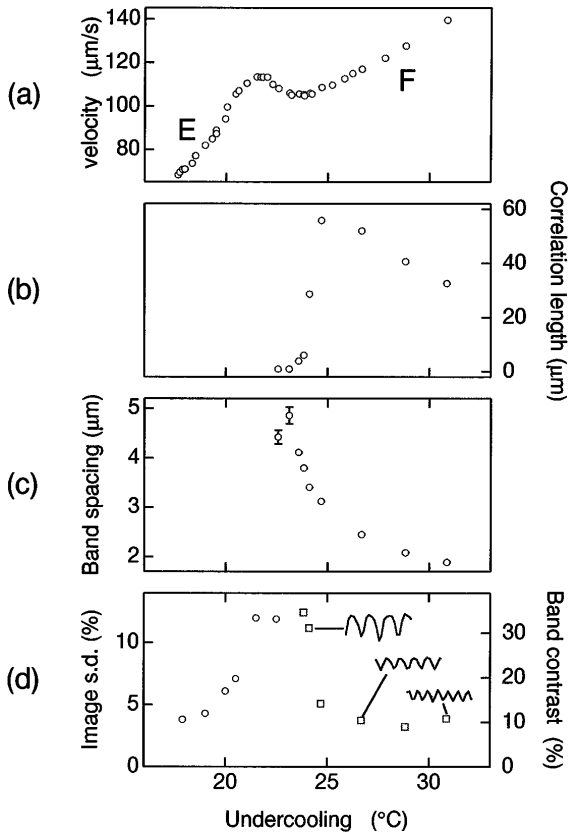

FIG. 5. The *EF* transition. (a) Growth velocity curve for modes *E* and *F*. (b) Correlation length of the bands (measured parallel to the growth direction). (c) Band spacing as a function of undercooling. (d) Measures of optical contrast. The circles on the left side of the plot indicate the standard deviation in image intensity measured in the unbanded regime. The points on the right show the average band amplitude in mode *F*. The insets show the evolution of the band profile throughout this region.

that intensity profiles become cusplike near the transition.) However, the sudden decrease in correlation length near the transition does not fit this scenario. Whatever the precise nature of this transition, the smooth variation in velocity, the lack of hysteresis in the data of Fig. 5 when the undercooling is varied about the transition point, and the divergence of intensity fluctuations on both sides of the transition—all of these identify it as second order.

The observation that banded spherulites are born in a second-order transition may be important for understanding the banding mechanism, which has remained one of the outstanding puzzles of crystal growth. Bands have been associated with a rotation in the optic axis of the radially arranged microcrystals making up the spherulite [3,17], which would then locally resemble the cholesteric liquid crystal phase. However, there is no agreement on the origin of this rotation or the mechanism responsible for creating large domains of correlated bands.

In summary, we have shown examples of several sharp morphology transitions in the solidification of 10 OCB in both the diffusive and kinetic regimes. These transitions have characteristics analogous to both first- and second-order phase transitions. In two cases (AB' and $B'B$), we see a jump in growth velocity, as expected for first-order morphology transitions. We have identified, both experimentally and theoretically, weakly first-order transitions (CD and DE) in which the velocity is continuous but the growth morphology changes sharply. Finally, the transition from unbanded to banded spherulitic growth (EF) is the first example of a second-order morphology transition, showing critical behavior and pretransitional effects.

We are grateful to J. Stavans for hospitality while the manuscript was written and to D. Allender, D. Kandel, and D. Mukamel for helpful conversations. This work was supported by NSERC (Canada).

*Present address: Exxon Research and Engineering Company, Route 22 East, Annandale, NJ 08801.

[1] E. Brener, H. Müller-Krumbhaar, and D. Temkin, Phys. Rev. E **54**, 2714 (1996).
[2] P. J. Phillips, in *Handbook of Crystal Growth, Vol. 2*, edited by D. T. J. Hurle (Elsevier, Amsterdam, 1993), Chap. 18.
[3] G. Ryschenkow and G. Faivre, J. Cryst. Growth **87**, 221 (1988); B. Miao, D. O. Northwood, W. Bian, K. Fang, and M. H. Fan, J. Mater. Sci. **29**, 255 (1994).
[4] J. Lipton, W. Kurz, and R. Trivedi, Acta Metall. **35**, 957 (1987).
[5] J. D. Hoffman, Polymer **24**, 3 (1983).
[6] E. Ben-Jacob, P. Garik, T. Mueller, and D. Grier, Phys. Rev. A **38**, 1370 (1988); E. Ben-Jacob and P. Garik, Nature (London) **343**, 523 (1990); O. Shochet and E. Ben-Jacob, Phys. Rev. E **48**, R4168 (1993).
[7] E. A. Brener and D. E. Temkin, JETP **82**, 559 (1996).
[8] Y. Saito and H. Müller-Krumbhaar, Phys. Rev. Lett. **74**, 4325 (1995).
[9] K. Eckler, R. F. Cochrane, D. M. Herlach, B. Feuerbacher, and M. Jurisch, Phys. Rev. B **45**, 5019 (1992); R. Willnecker, D. M. Herlach, and B. Feuerbacher, Phys. Rev. Lett. **62**, 2707 (1989).
[10] D. Grier, E. Ben-Jacob, R. Clarke, and L. M. Sander, Phys. Rev. Lett. **56**, 1264 (1986).
[11] J. S. Langer, Science **243**, 1150 (1989).
[12] J. L. Hutter and J. Bechhoefer, Physica (Amsterdam) **239A**, 103 (1997).
[13] J. L. Hutter, Ph.D. thesis, Simon Fraser University, 1997.
[14] J. Krug and H. Spohn, in *Solids Far From Equilibrium*, edited by C. Godrèche (Cambridge University Press, Cambridge, 1992), pp. 479–582.
[15] C. N. R. Rao and K. J. Rao, *Phase Transitions in Solids* (McGraw-Hill, London, 1978), pp. 120–133.
[16] P. G. de Gennes and J. Prost, *The Physics of Liquid Crystals* (Clarendon Press, Oxford, 1993), pp. 286–293.
[17] A. Keller, J. Polym. Sci. **17**, 291 (1955).